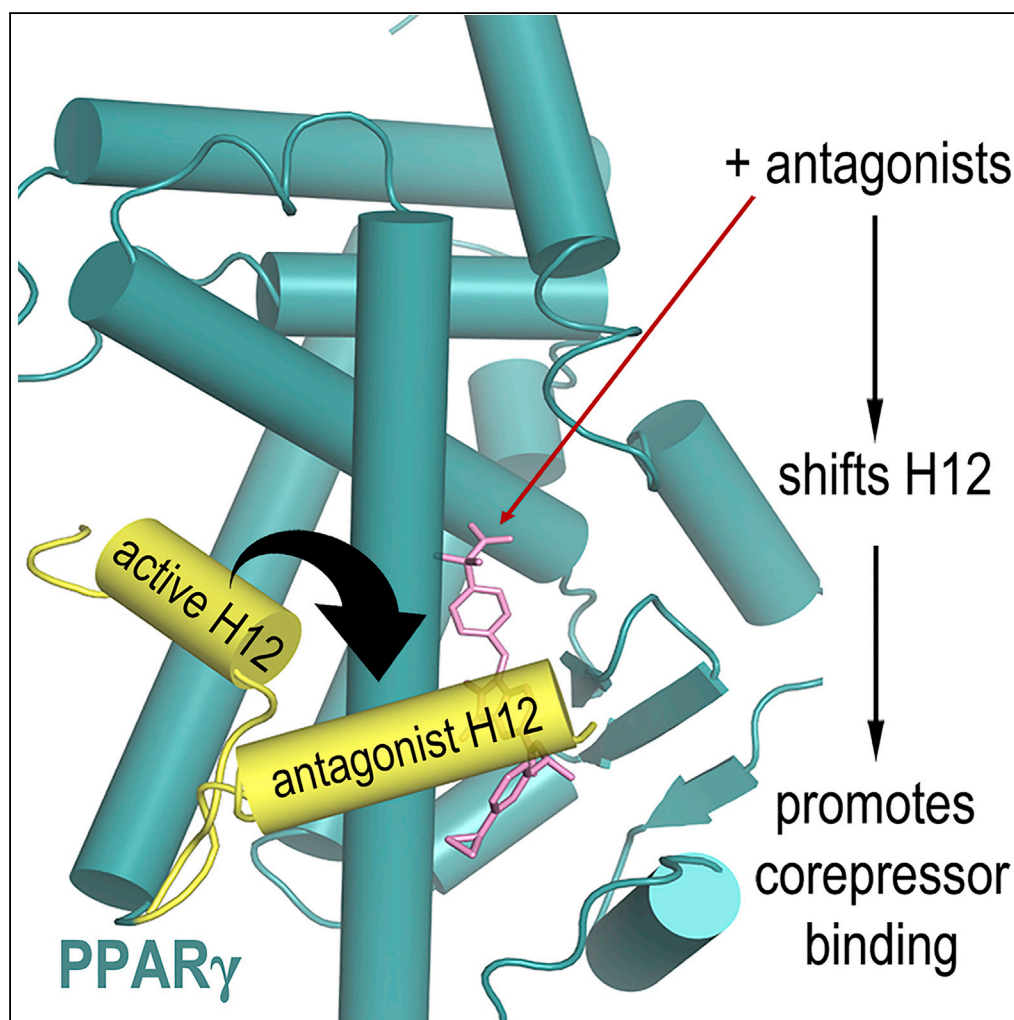**Article**

PPARγ in Complex with an Antagonist and Inverse Agonist: a Tumble and Trap Mechanism of the Activation Helix

Rebecca L. Frkic, Andrew C. Marshall, Anne-Laure Blayo, Tara L. Pukala, Theodore M. Kamenecka, Patrick R. Griffin, John B. Bruning

john.bruning@adelaide.edu.au

HIGHLIGHTS

SR10171 and SR11023 bind PPARγ LBD and "pull" H12 to an antagonist conformation

H12 movement is mechanistically distinct from PPARα and other nuclear receptors

The antagonist conformation of H12 enables corepressor binding

Mechanism of antagonism key to improving T2DM treatments

Article

PPARγ in Complex with an Antagonist and Inverse Agonist: a Tumble and Trap Mechanism of the Activation Helix

Rebecca L. Frkic,[1] Andrew C. Marshall,[1] Anne-Laure Blayo,[3] Tara L. Pukala,[2] Theodore M. Kamenecka,[3] Patrick R. Griffin,[3] and John B. Bruning[1,4,*]

SUMMARY

Peroxisome proliferator activated receptor γ (PPARγ) is a nuclear receptor and target for antidiabetics that increase insulin sensitivity. Owing to the side effects of PPARγ full agonists, research has recently focused on non-activating ligands of PPARγ, which increase insulin sensitivity with decreased side effects. Here, we present the crystal structures of inverse agonist SR10171 and a chemically related antagonist SR11023 bound to the PPARγ ligand-binding domain, revealing an allosteric switch in the activation helix, helix 12 (H12), forming an antagonist conformation in the receptor. H12 interacts with the antagonists to become fixed in an alternative location. Native mass spectrometry indicates that this prevents contacts with coactivator peptides and allows binding of corepressor peptides. Antagonists of related nuclear receptors act to sterically prevent the active configuration of H12, whereas these antagonists of PPARγ alternatively trap H12 in an inactive configuration, which we have termed the tumble and trap mechanism.

INTRODUCTION

Peroxisome proliferator activated receptor γ (PPARγ) is a ligand-activated nuclear receptor that plays key roles in human metabolism and glucose homeostasis (Bruning et al., 2007; Kroker and Bruning, 2015; Taygerly et al., 2013; van Marrewijk et al., 2016). The receptor performs its function through obligate heterodimerization with retinoid X receptor α (RXRα) to form a transcription factor capable of binding to peroxisome proliferator response elements (PPRE) on DNA to initiate transcription of target genes (Chandra et al., 2008). There are over 100 target genes of PPARγ, which include genes involved in fatty acid metabolism, glucose homeostasis, and adipogenesis. Endogenous ligands of PPARγ include fatty acids, eicosanoids, and lipid metabolites.

PPARγ has been the target of pharmaceuticals that have generated billions of dollars (USD) as antidiabetics. The activity of PPARγ is central to glucose homeostasis through modulating the response to insulin, and a dysregulation in PPARγ signaling contributes to the onset and perpetuation of type 2 diabetes. A major class of antidiabetic treatments targeting PPARγ is the thiazolidinedione (TZD) class of compounds, which are synthetic full agonists of the receptor. These compounds have previously been effective in treating symptoms of type 2 diabetes, but their use has been restricted because of significant side effects, resulting in their limited clinical use. These side effects are caused by supraphysiological activation of PPARγ-controlled genes, which dysregulate normal metabolic processes and include congestive heart failure, weight gain, loss of bone mineral density, and renal fluid retention leading to edema (Bruning et al., 2007; Choi et al., 2011; Wakabayashi et al., 2011). Phosphorylation of PPARγ at Ser273 by Cdk5-regulated ERK has been shown to correlate with obesity and insulin resistance, and PPARγ ligands that improve insulin sensitivity block this phosphorylation, resulting in PPARγ target genes returning to a homeostatic state (Banks et al., 2015; Choi et al., 2010, 2011). Antagonists of PPARγ have been established as promising alternatives to full agonists as clinically applicable antidiabetic agents (Choi et al., 2011, 2016; Marciano et al., 2015a, 2015b; Stechschulte et al., 2016). These compounds that bind PPARγ restore insulin sensitivity without causing side effects associated with the activation of the receptor (Choi et al., 2011).

PPARγ is composed of an intrinsically disordered N-terminal AF1 domain (activation function 1 domain) that binds co-regulators; a zinc-finger domain for DNA binding (DBD); a ligand-binding domain (LBD), which includes the AF2 (activation function 2) that binds ligands and co-regulators; and a mobile hinge region that

[1]Institute for Photonics and Advanced Sensing (IPAS), School of Biological Sciences, The University of Adelaide, Adelaide, SA 5005, Australia

[2]School of Physical Sciences, The University of Adelaide, Adelaide, SA 5005, Australia

[3]Department of Molecular Medicine, The Scripps Research Institute, Jupiter, FL 33458, USA

[4]Lead Contact

*Correspondence: john.bruning@adelaide.edu.au

joins the LBD and DBD. The crystal structure of the PPARγ LBD in the presence of agonist ligands shows that the domain conforms to the canonical nuclear receptor LBD architecture, consisting of 13 α-helices (1–12 and 2′) and a small β-sheet (Nolte et al., 1998). The AF2 coactivator-binding surface, which is critical for determining the transcriptional output of PPARγ through differential recruitment of co-regulators, comprises helices H3–H5 and H12, with H12 oriented toward the space between H11, H4, and the H8-H9 interconnecting loop. PPARγ agonists stabilize H12 as part of the AF2 surface through a network of hydrogen bonds with H12 to stabilize the helix in a position ideal for interacting with the AF2 as well as coactivators (Nolte et al., 1998). Surprisingly, all crystal structures of the PPARγ LBD to date, including the apo-LBD, have shown H12 in this same "active" conformation. This puzzle was resolved by studies of the dynamics of the LBD, which indicate that the LBD, and particularly H12, is highly mobile in the apo structure. Although no atomic-level structure has been produced using nuclear magnetic resonance (NMR), the apo receptor produced few peaks in 3D HNCO spectra, indicating that the LBD undergoes large levels of molecular motion when not bound to ligand (Johnson et al., 2000). In contrast, when the full agonist rosiglitazone was added, the LBD was largely stabilized, showing much less molecular motion overall. Further work using hydrogen-deuterium exchange (HDX) confirmed these results, showing that full agonists, including rosiglitazone, strongly and selectively stabilize H12 and H3, in contrast to partial agonists and antagonists (Bruning et al., 2007; Choi et al., 2010; Hamuro et al., 2006). From this, it was hypothesized that the mechanism of action of full agonists is to strongly stabilize the AF2 surface through H12, allowing less of an entropic penalty for coactivator binding leading to full transcriptional output. This mechanism of stabilizing an active configuration of a mobile H12 is like that observed in related nuclear receptors, such as estrogen receptor α (ERα), estrogen receptor β (ERβ), and PPARα. It then seemed to follow that antagonists would destabilize the H12 interaction, as seen with ERα, ERβ, and PPARα, allowing corepressors to bind the corepressor-binding cleft, blocking agonism by not allowing coactivators to bind. Our group recently showed that in the apo form, H12 exchanges between many conformations (Chrisman et al., 2018). Several agonists and inverse agonists conformationally constrain H12 into states that favor coregulator binding (Chrisman et al., 2018). The dynamic nature of H12 has been further investigated using chemical cross-linking mass spectrometry (MS), which revealed that, when the LBD is in the apo state, H12 samples a dynamic ensemble of distinct conformers, including an antagonist conformation, which is stabilized upon the addition of an antagonist (Zheng et al., 2018). These studies demonstrated that, in solution, H12 in the antagonist bound form of PPARγ is located near the H2-H3 region of the LBD (Zheng et al., 2018). However, no such antagonist locked state of H12 has been discovered in crystal structures of PPARγ to date, leaving the exact atomic details of the antagonist and inverse agonist bound forms of PPARγ undetermined.

Given the promise of antagonists of PPARγ in the treatment of type 2 diabetes and certain cancer types (Khandekar et al., 2018), it is important to understand their mechanism of action. For related receptors, such as ERα, ERβ, and PPARα, bound antagonists sterically clash with H12 in the active configuration (Brzozowski et al., 1997; Pike et al., 1999; Srinivasan et al., 2017; Xu et al., 2002). We have termed this the "push and tumble mechanism" in which the antagonists bound to these LBDs sterically clash with H12 (the "push") and destabilize it in solution (the "tumble"). However, in the existing X-ray crystal structures of antagonists bound to the LBD of PPARγ, H12 is in the agonist-like active conformation. This is possibly due to coactivator peptides present forcing the complex to the active state or studies using ligands that are known to adopt multiple conformations within the binding pocket in solution. Thus, although the PPARγ antagonists appear differently from antagonists of related receptors, as they do not sterically block the active H12 conformation, the allosteric switches required for corepressor binding remain unclear.

To further investigate the mechanism of antagonism in PPARγ, we obtained X-ray crystal structures of the PPARγ LBD bound to two separate chemical antagonists, SR10171 and SR11023 (Figure S1), in the absence of other peptides. Both compounds are a result of modification of the indole scaffold of SR1664, which improves its pharmacokinetic properties (Stechschulte et al., 2016; Zheng et al., 2018). SR10171 partially represses basal transcriptional activity of PPARγ, classifying it as a partial inverse agonist (Stechschulte et al., 2016), whereas SR11023 displays no transcriptional activity, classifying it as an antagonist (Zheng et al., 2018) in transcriptional reporter assays. Both display high-affinity binding to the receptor, with SR10171 having an IC_{50} of 220 nM and SR11023 having an IC_{50} of 108 nM in a competition displacement assay (PPARγ Lantha Screen) (Zheng et al., 2018). Both compounds compete with the full agonist rosiglitazone and right-shift its EC_{50} (Zheng et al., 2018). In addition, both compounds display insulin-sensitizing properties. SR10171 possessed similar insulin-sensitizing efficacy as TZDs and SR1664 in obese diabetic mice (Stechschulte et al., 2016) and in addition modulated osteoblast, osteocyte, and osteoclast activities,
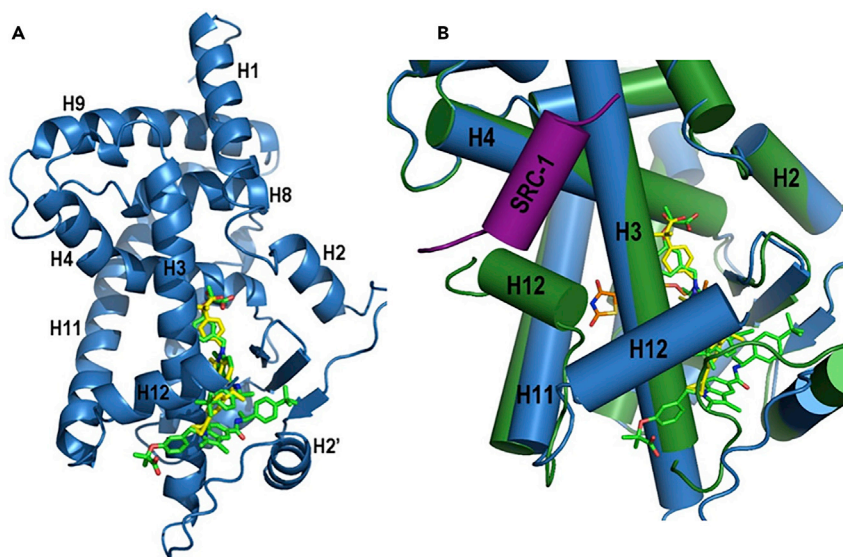
Figure 1. Crystal Structures of SR10171 and SR11023 Bound to PPARγ LBD

PPARγ LBD main chain is shown in blue, with ligands shown as green (SR10171) and yellow (SR11023) sticks.

(A) Superposition of both ligand-bound structures.

(B) Comparison of crystal structures (blue) with rosiglitazone (orange sticks)-bound PPARγ LBD (dark green) demonstrates the change in helix 12 conformation. Nuclear receptor coactivator SRC-1 is shown in purple (PDB: 2PRG).

indicating an anabolic effect on bone. Interestingly, SR10171 was a partial agonist in GAL-4 transactivation reporter assays of PPARα with an EC_{50} of 1 μM (Stechschulte et al., 2016). SR11023 showed pS273 blocking capabilities, consistent with antidiabetic properties of PPARγ ligands (Zheng et al., 2018).

X-ray co-crystal structures of PPARγ with these ligands reveal that H12 adopts a non-agonist-like conformation, stabilized by interactions with the antagonist or inverse agonist bound in the ligand pocket. Unlike antagonists of the ERα, ERβ, and PPARα receptors, these ligands do not appear to sterically clash with an agonist H12 conformation but rather trap it in an alternative conformation: a hold away mechanism (tumble and trap), rather than a push away mechanism (push and tumble). Native MS supports the idea that the alternative H12 conformation inhibits transcription by removing important contacts with coactivators, making the AF2 interaction interface accessible to corepressors.

RESULTS

SR10171 and SR11023 Induce an Alternate H12 Conformation in PPARγ LBD

Co-crystal structures were obtained for both SR10171 and SR11023 bound to the PPARγ LBD (Figure 1A), with data refinement statistics in Table 1. The structures were solved in space group P6₅22 in both cases; this is the first instance of this crystal form of PPARγ. The asymmetric unit contained one subunit of the PPARγ LBD (monomeric). Most of the LBD (H1–H11) conformed to the canonical PPARγ LBD structure, with negligible variation in the global LBD fold compared with previous structures (root-mean-square deviation [RMSD] of 0.71 Å across 238 Cα atoms and 0.69 Å RMSD over 234 Cα atoms compared with rosiglitazone-bound PPARγ LBD, PDB: 2PRG). Superimposition of the crystal structures with each other demonstrates their high similarity, with an RMSD of 0.50 Å over 265 Cα atoms.

Remarkably, the structures indicate an alternative conformation of H12, resembling an antagonist nuclear receptor structure conformation, where H12 (residues following Leu465) is on the outside face of H3 extending toward the H2'-H3 connecting loop distal to the remainder of the LBD (Figure 1B). This orientation is the first structural evidence of an antagonist H12 conformation in PPARγ.

The active conformation of H12 has been shown to be key for stabilizing the AF2 region to enable coactivator binding. When in the agonist conformation, H12 is stabilized as part of the AF2 coactivator-binding surface by agonists of PPARγ, which bind across H3, between H3 and H7, and extend toward the AF2

Parameter	SR10171	SR11023
PDB accession code	6C5Q	6C5T
Space group	P 6_5 2 2	P 6_5 2 2
Cell dimensions		
a, b, c (Å)	65.19, 65.19, 368.45	63.64, 63.64, 365.35
α, β, γ (°)	90, 90, 120	90, 90, 120
Resolution range (Å)	61.4–2.4 (2.5–2.4)	19.7–2.75 (2.9–2.75)
R_{merge} (%)[a]	8.9 (5.6)	8.4 (4.1)
R_{pim} (%)	6.7 (82)	8.0 (83)
Mean (I)/σ(I)	40.6 (1.5)	31.0 (1.6)
Completeness	99.0 (98.1)	97.8 (95.4)
Multiplicity	53.4 (55.4)	18.8 (19.9)
Structure refinement		
Resolution range (Å)	41.6–2.4	19.7–2.75
Unique reflections	19,215 (1,837)	12,275 (1,165)
R_{work}[b]	0.249 (0.38)	0.254 (0.41)
R_{free}[c]	0.277 (0.423)	0.286 (0.402)
Total number of		
Non-hydrogen atoms	2,293	2,150
Protein atoms	2,179	2,039
Ligand atoms	80	38
Water molecules	34	73
RMSD		
Bond length (Å)	0.002	0.001
Bond angle (deg)	0.45	0.38
B-factors (Å^2)		
Overall	75.57	97.27
Average protein atoms	76.13	98.04
Average ligand atoms	68.64	90.96
Average solvent	55.63	78.83

Table 1. Crystallographic Data Statistics
Values in parentheses correspond to the last shell.
[a]$R_{merge} = \Sigma |I - < I > |/\Sigma I$.
[b]$R_{work} = \Sigma |F_o - F_c|/\Sigma |F_o|$ for all data excluding data used to calculate R_{free}.
[c]$R_{free} = \Sigma |F_o - F_c|/\Sigma |F_o|$, for all data.

surface (Bruning et al., 2007; Nolte et al., 1998). Crystal structures of PPARγ LBD bound to full agonist rosiglitazone show that the thiazole head group of rosiglitazone forms a network of hydrogen bonds with His323 of H4, His449 of H11, and Tyr473 of H12, residues that constitute the AF2 surface (Chandra et al., 2008; Gampe et al., 2000; Gelin et al., 2015; Liberato et al., 2012; Nolte et al., 1998). These interactions mediated by TZDs stabilize the AF2 surface, strengthened by a hydrogen bond between His323 of H4 and Tyr473 of H12 (Nolte et al., 1998). H12 is central to this stabilizing network, enabling binding of
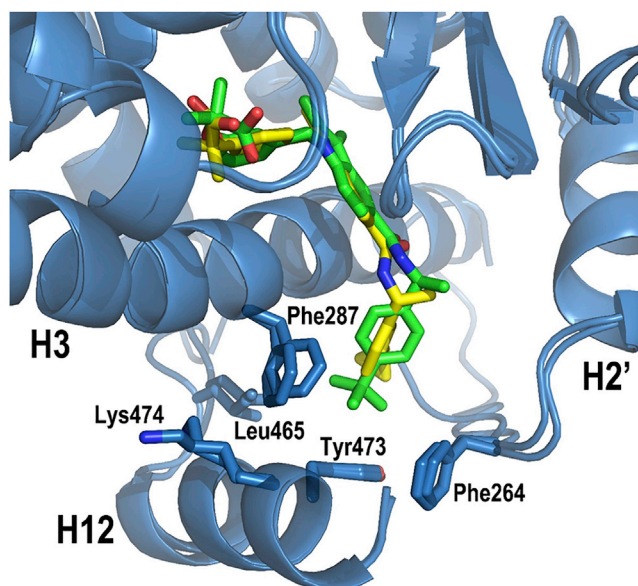
Figure 2. Hydrophobic Interactions Stabilizing H12 in the Antagonist Conformation

The hydrophobic tails of SR10171 (green sticks) and SR11023 (yellow sticks) mediate hydrophobic interactions between H3 and H12 of the PPARγ LBD (blue ribbons) to stabilize H12 at H3, away from the AF2 coactivator-binding surface. Contributing hydrophobic residues are labeled and shown as sticks.

transcription-promoting coactivators to the AF2 surface. In the SR10171/SR11023 structures, the ligands are bound in the binding pocket distal to the AF2 surface, lacking direct interactions with constituents of the AF2 surface. This leaves H12 unrestrained by the stabilizing AF2 network, with the remainder of the AF2 making no contacts with the ligand and forming a conformation nearly identical to the apo state structure. Specifically, H12 in these structures is held in place by a hydrophobic network composed of four constituents: (1) the hydrophobic tail of SR10171 or SR11023; (2) side chains from loop regions surrounding H3 and H12, including residues Phe264 and Leu465; (3) H12 residue side chains, including Tyr473 and Lys474; and (4) H3 residue side chains Phe287 and Gly284. H12 is also held in place by one hydrogen bond in both structures: Tyr477 side chain to Glu291 side chain (2.6 Å) for the SR10171 co-structure and Gln283 side chain to the backbone oxygen atom of Ser464 (3.2 Å) in the SR11023-bound structure. The hydrophobic interactions stabilizing H12 can be viewed in Figure 2.

SR10171 and SR11023 Exhibit Unique Ligand-Binding Modes

Both the SR10171- and SR11023-bound crystal structures showed that ligand interaction is mostly through hydrophobic interactions within the ligand-binding pocket, contributed by Ile262, Phe287, Leu330, Leu333, Ile341, Ser342, and Tyr473. Both ligands are positioned between H3 and the beta sheet and wrap around the solvent-exposed face of H3. Difference Fourier electron density in the ligand-binding pocket of the SR10171-bound crystal structure showed that a second SR10171 ligand was bound simultaneously (refined to 88% occupancy) and does not overlap with the binding pose of the first SR10171 conformation. This could be a result of excessive ligand concentration (10 mM) during co-crystallization. Experiments to define the lower affinity binding constant for the second binding event were unsuccessful owing to the hydrophobic nature of the compounds and the inability to keep them in solution at such high concentrations. The presence of the additional SR10171 ligand appears to have no effect on the global fold of the LBD including H12 compared with SR11023-bound PPARγ LBD.

In addition to hydrophobic interactions, some residue-specific interactions were made between the ligands and the receptor (Figure 3). The terminal carboxyl of the higher occupancy SR10171 ligand forms a 2.6 Å salt bridge with Arg288, and the carbonyl forms a 3.0 Å hydrogen bond with the amide of the lower occupancy ligand, which forms a 3.1 Å hydrogen bond with His266. SR11023 forms a π-π interaction with Phe287 in addition to hydrophobic interactions. Composite omit electron density maps of the ligands modeled to the data can be found in Figure S2.
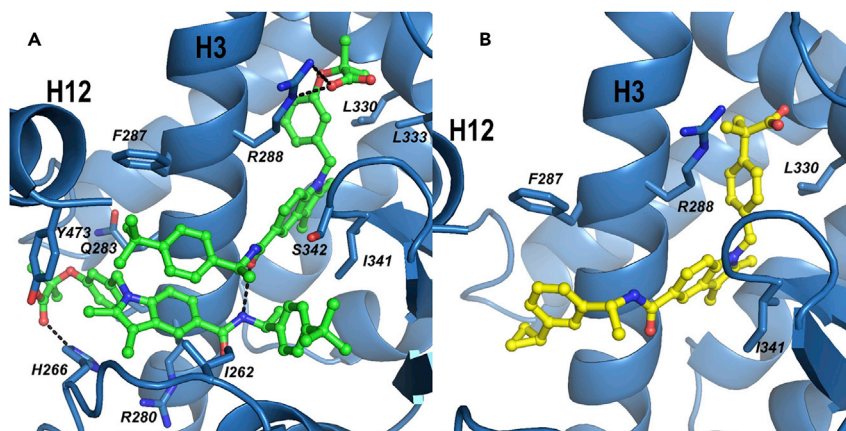
Figure 3. SR10171 and SR11023 Exhibit Unique Ligand-Binding Modes

Crystal structures reveal ligand-binding modes of (A) SR10171 (green sticks) and (B) SR11023 (yellow sticks) bound to PPARγ LBD (blue ribbons). The side chains of the major contributing residues are shown as blue sticks.

Antagonists of PPARγ Do Not Prevent LBD-Dependent Heterodimerization of PPARγ with RXRα

PPARγ performs its active function through obligate heterodimerization with RXRα, where the two nuclear receptors dimerize through their ligand-binding domains as well as in a DNA-dependent manner at their DBDs (Chandra et al., 2008; Issemann et al., 1993; Kojetin et al., 2015). Interestingly, our structures were monomeric in the crystal lattice, in contrast to other PPARγ structures, which are monomeric only in the presence of coactivator peptide. The PPARγ LBD ordinarily forms a homodimer upon crystallization in a manner analogous to PPARγ/RXRα LBD heterodimerization. Prompted by the uniquely monomeric crystal structures, we hypothesized that SR10171 and SR11023 could potentially be exhibiting their repressive characteristics by disrupting the LBD-dependent heterodimerization between PPARγ and RXRα, which is required for transcription of target genes. Native MS is well established to report on the stoichiometry of protein assemblies with excellent correlation to solution phase properties (Liko et al., 2016). We therefore investigated PPARγ/RXRα LBD heterodimerization in the presence of antagonists using native MS, which showed that the heterodimer remained intact upon addition of antagonist or inverse agonist (Figure 4). This was indicated by the relative abundance of the free monomers remaining unchanged compared with the apo spectra, considering the population of the heterodimer in the presence of antagonists is in both apo and holo forms. The spectra also reveal an abundant holo heterodimer species in all cases of ligand addition, suggesting that PPARγ can bind to the ligands while in complex with RXRα LBD. Native PAGE of PPARγ and RXRα LBDs with increasing concentrations of SR10171 or SR11023 yielded results consistent with native MS (Figure S3). Both methods demonstrated a consistent abundance of complexes corresponding to the PPARγ/RXRα LBD heterodimer even at high ligand concentrations. This evidence suggests that SR10171 and SR11023 do not disrupt heterodimerization between PPARγ and RXRα LBDs, and that repression of PPARγ activity by the ligands must occur through an alternate mechanism. This discovery indicates the importance of higher order regulation of the PPARγ transcriptional complex beyond interaction with RXRα, particularly the recruitment of coactivators and corepressors to the PPARγ/RXRα transcriptional complex.

SR10171 and SR11023 Cause Preferential Recruitment of Corepressors to PPARγ

The recruitment of coactivators and corepressors is central to the regulation of transcription factor activity (DiRenzo et al., 1997). As such, the conformation of H12 induced by SR10171 and SR11023 in the co-crystal structures suggested a distinct binding site on the surface of PPARγ that would enable corepressor binding. Native MS was employed to investigate antagonist and inverse agonist binding to the PPARγ/RXRα LBD heterodimer in the presence of coregulator peptides (Figure 4).

We used a coactivator peptide (SRC) and two corepressor peptides (SMRT and NCOR), as well as ligands SR10171, SR11023, and rosiglitazone, to determine the effects of these ligands on coregulator binding. It can be observed that, for all cases of peptide addition to the heterodimer in the absence of ligand (the bottom spectra of each panel), there was an abundance of peptide-bound heterodimer (light green), suggesting that each of the peptides can bind with sufficient affinity to the heterodimer in the absence of ligands. In
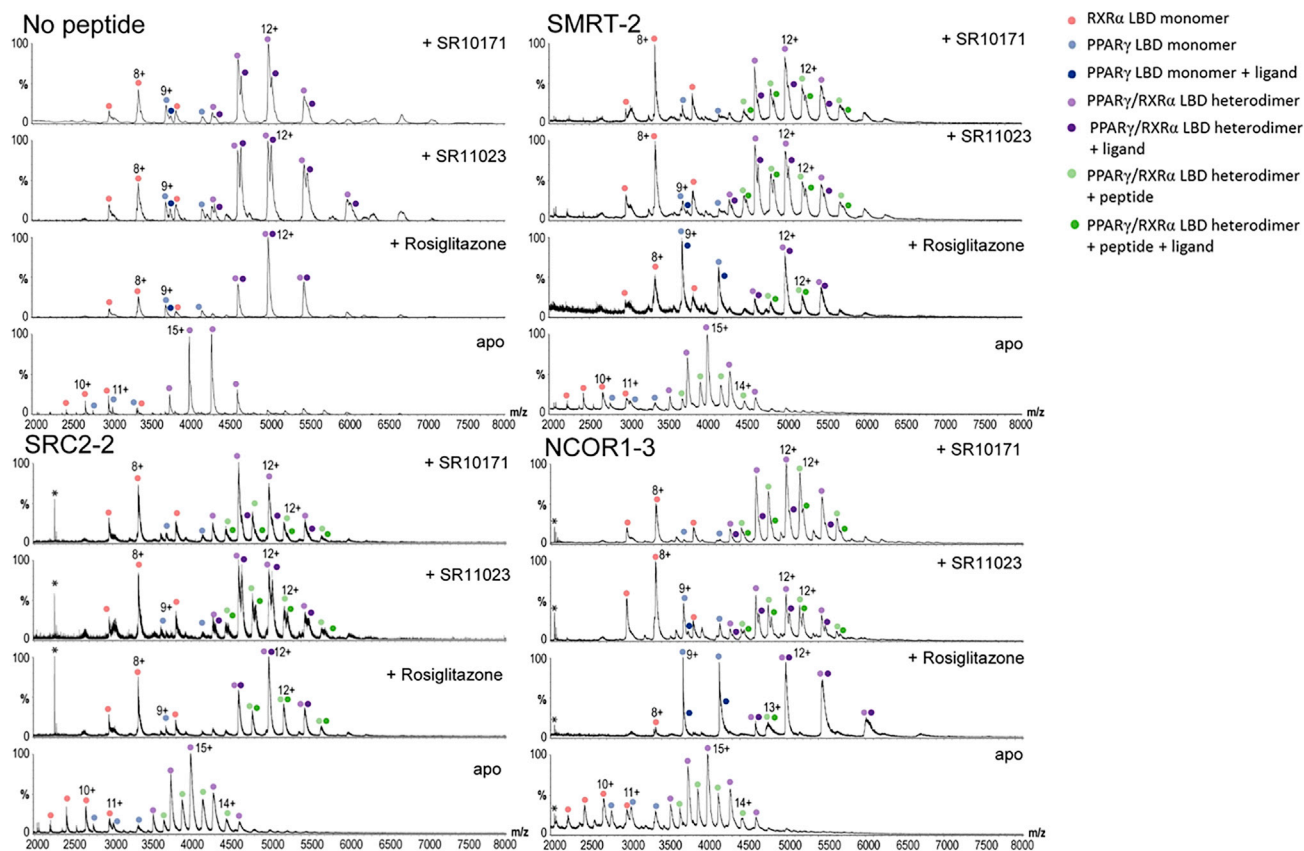
Figure 4. Native Mass Spectrometry Shows the Effect of Ligand Binding on PPARγ/RXRα LBD Heterodimerization as well as Coregulator Peptide Recruitment

Native mass spectrometry was performed on the PPARγ/RXRα LBD heterodimer in the presence of SR10171, SR11023, or rosiglitazone. In the absence of coregulator peptides, the spectra showed significant abundance of antagonist-bound heterodimer, and minimal change in the amount of free monomer upon addition of antagonist, suggesting no disruption of the heterodimer upon ligand addition. Corepressor peptides NCOR1-3 and SMRT-2 and coactivator peptide SRC2-2 were added to PPARγ/RXRα LBD heterodimer to elucidate the coregulator binding capabilities of the holo heterodimer. Ligands and peptides were added to heterodimer as labeled in a 1:1:1 molar ratio. Unbound coregulator peptides are denoted (*).

the case of SRC, when ligand was added the SRC coactivator peptide was still able to bind, as indicated by the presence of the dark green species corresponding to the peptide-bound holo heterodimer. This was less abundant in the case of SR10171, where the abundance of this species was lesser compared with the other spectra in this panel, suggesting that SR10171 does not bind as strongly to the SRC-bound heterodimer, consistent with its function as an inverse agonist.

Analysis of the SMRT/NCOR spectra shows that compared with the apo spectra, there was a minimal abundance of corepressor and rosiglitazone-bound species, as indicated by a negligible abundance of the dark green species, particularly for NCOR. There appeared to be an abundant presence of corepressor and SR10171/SR11023-bound heterodimer, suggesting that SR10171 and SR11023 strongly encourage corepressor binding.

These findings suggest that distinct coregulator recruitment profiles is a key factor in the mechanism of antagonism of PPARγ. The preferential recruitment of corepressors over coactivators by our compounds leads to repressive effects on the transcription of PPARγ-controlled genes.

DISCUSSION

Understanding the details of PPARγ modulation by ligands is critical for obtaining effective insulin sensitization while limiting the incidence of adverse side effects due to superfluous activation of the receptor. It has been made evident that antagonists and inverse agonists are the most promising approach as

antidiabetic agents for their abilities to normalize insulin sensitivity while minimizing PPARγ transactivation and hence minimizing side effects.

Crystal structures of PPARγ LBD to date have demonstrated a conserved backbone fold with little variation in H12 (Bruning et al., 2007; Hughes et al., 2012). We hypothesize that the lack of a distinct antagonist structure in PPARγ found to date could be due to one or more of the following reasons: (1) crystal artifacts that stabilize H12 in the agonist conformation are very common in PPARγ LBD co-crystal structures, (2) several of the antagonist-bound PPARγ structures have bound coactivator peptides that force H12 in the agonist conformation, (3) PPARγ ligands have been found to bind in more than one conformation in solution studies but are generally locked in one conformation in crystal structures and this may have precluded the ability to see the H12 destabilized version of the structure, and (4) there may be multiple and/or different mechanisms of antagonism in PPARγ with only a certain class having been captured in the few antagonist-bound PPARγ structures solved to date.

We have obtained crystal structures of an inverse agonist and an antagonist bound to PPARγ LBD, which show H12 in an alternate orientation similar to antagonist conformations reported in other nuclear receptors. The attainment of these crystal structures overcomes the hurdles stated previously that have thus far prevented crystal structures being solved with H12 in the antagonist position. The absence of a coactivator peptide as well as crystallization in a space group novel to PPARγ LBD has enabled the resolving of the antagonist H12 conformation in PPARγ. This has important implications in the field of PPARγ research, as it provides the first structural insight into the mechanism of antagonism in PPARγ as a result of modulation by non-activating ligands.

The consequences of the antagonist H12 conformation appear to have a direct effect on coregulator recruitment, as exhibited by our native MS data that showed a minimal presence of SR10171/SR11023-bound heterodimer complexed with coactivator peptide. The structural mechanism behind this can be hypothesized by analyzing the crystal structure of the active complex: PPARγ LBD bound to rosiglitazone and coactivator peptide. Previous crystal structures of PPARγ LBD bound to coactivator peptide have demonstrated essential interactions between the peptide and AF2 of PPARγ. Residues of H12 are critical for making interactions with the LXXLL motif of nuclear receptor coactivators (Nolte et al., 1998). A highly conserved Glu471 of H12 in nuclear receptors is involved in an extensive hydrogen bond network with residues of the coactivator peptide, as well as participating in a charge clamp alongside Lys301 of H3 to lock the coactivator peptide in place (Nolte et al., 1998). This highlights the importance of H12 conformation for interacting with the remainder of the AF2 to stabilize this region, allowing coactivators to bind. The antagonist conformation of H12 in our crystal structures does not participate in the AF2 surface, excluding the formation of the essential hydrogen bond network normally contributed by Glu471 of H12 to lock the coactivator peptide in place. This abrogates coactivator binding in a physiological context, consistent with our native MS data.

In addition to this, our native MS data revealed that corepressor peptides were able to bind to the PPARγ/RXRα heterodimer in the presence of SR10171 or SR11023 and not when rosiglitazone was bound to the heterodimer. Superimposition of corepressor-bound PPARα LBD with SR10171, SR11023, and rosiglitazone-bound PPARγ crystal structures reveals a clash between the corepressor bound to PPARα and the active conformation of H12 of rosiglitazone-bound PPARγ (Figure S4). The antagonist conformation of H12 in PPARα results in a larger pocket to accommodate corepressor binding (Xu et al., 2002). This is pertinent to PPARγ, which shows an almost identical antagonist H12 orientation to PPARα when bound to SR10171 or SR11023. This suggests that, in the PPARγ system, SR10171 and SR11023 attract H12 to the antagonist conformation, which opens the corepressor-binding cleft to enable SMRT and NCOR binding to the receptor. This is a feasible reason for the abundant corepressor binding exhibited in the presence of SR10171 and SR11023 shown in native MS, as well as negligible binding of rosiglitazone to corepressor-bound heterodimer through steric clashing between corepressor and the active conformation of H12. This can be confirmed by obtaining a crystal structure of PPARγ bound to a corepressor, which should be the focus of future structural studies investigating antagonism in PPARγ. From the current data, it appears that the molecular mechanism of antagonism by these compounds is through preferential recruitment of corepressors over coactivators, thereby lowering activation of PPARγ target genes. Attempts were made to complement native MS using surface plasmon resonance but it was shown to be intractable owing to the hydrophobicity of the compounds.

The structural mechanism of PPARγ antagonism in our crystal structures differs from that of PPARα. What is most strikingly different between the PPARγ and the PPARα antagonist structures is the differing ligand-binding modes. In the case of PPARα, GW6471 wraps around the buried surface of H3 and extends toward
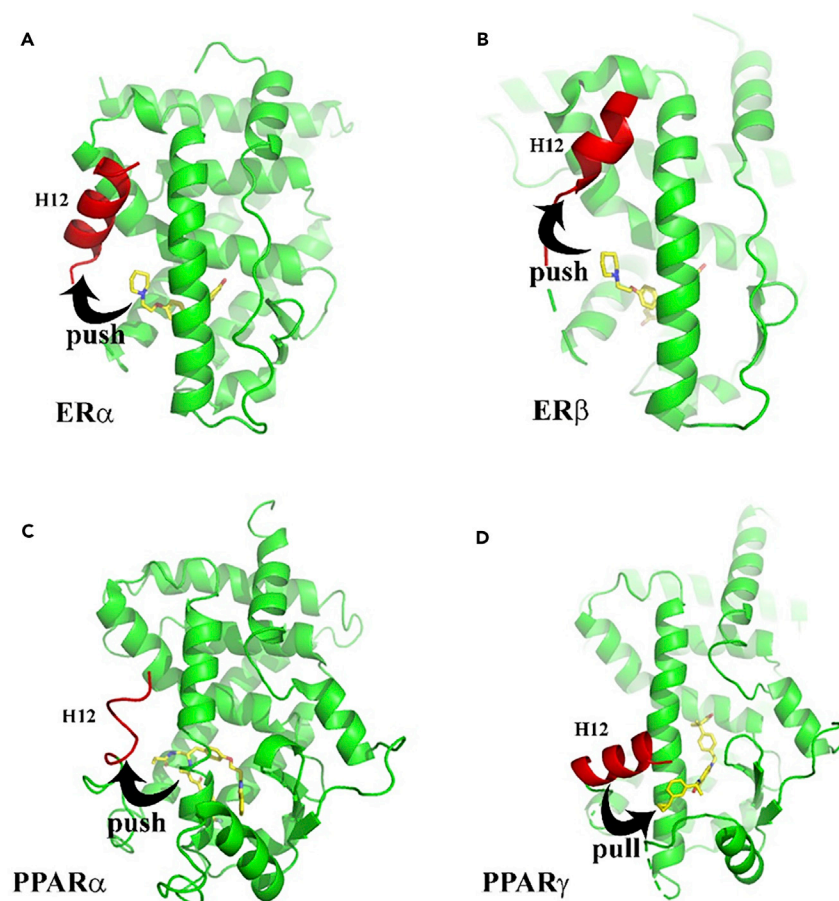
Figure 5. PPARγ H12 Shifts to the Antagonist Conformation in a Mechanistically Distinct Manner to Other Nuclear Receptor LBDs

Protein molecules are shown as green ribbons, with helix 12 highlighted in red. Respective ligands are shown as yellow sticks.

(A–C) (A) ERα bound to antagonist Raloxifene (PDB: 1ERR), (B) ERβ bound to Raloxifene (PDB: 1QKN), and (C) PPARα bound to antagonist GW6471 show that steric clashing by the ligands pushes H12 into the antagonist conformation.

(D) Our crystal structures of PPARγ bound to antagonists show that the ligands pull H12 into the antagonist conformation, a novel mechanism distinct from other nuclear receptors.

the space usually occupied by the active H12 conformation, as well as occupies the space near the β-sheet. This contrasts with our crystal structures, where SR10171 and SR11023 are positioned entirely within the β-sheet side of H3, making no contacts with the region of the binding pocket closest to the AF2 surface. Crystal structures of PPARα, ERα, and ERβ bound to antagonists show that H12 shifts to the antagonist conformation through steric clashing between the ligand and the active H12 conformation, where the antagonist forces H12 out of the active position (Brzozowski et al., 1997; Shiau et al., 1998; Xu et al., 2002). The crystal structure of PPARα bound to antagonist GW6471 shows that the ligand protrudes out of the space between H3 and H11 to sterically clash with H12, forcing it out of the active position and into a dynamic and destabilized state, to the point where the secondary structure of the helix has been distorted in the crystal structure for this region. In our crystal structures of PPARγ, SR10171 and SR11023 do not occupy the space between H3, H12, and H11 in PPARγ to force H12 out of the active conformation but are instead located between H3 and the β-sheet to "pull" H12 into the antagonist conformation (Figure 5). We have hypothesized that PPARγ antagonism operates via a "tumble and trap" mechanism, where "tumble" refers to the dynamic nature of H12 in solution in the absence of ligand, where upon the addition of SR10171 or SR11023 H12 is "trapped" in the antagonist conformation mediated by interactions with the ligands. This is mechanistically distinct from PPARα and highlights the uniqueness of SR10171 and SR11023 in their ligand-binding modes to exert their non-activating properties. In both cases, the resulting

outcome of the ligands despite their mechanisms is that H12 can move away from the AF2 surface, which opens up the corepressor-binding cleft. This suggests some conservation in the mechanism of antagonism through the structural consequences of H12 conformation in PPARs, independent of the underlying mechanism that results in the allosteric shift in H12.

Our findings reveal what may be only one mechanism of antagonism in PPARγ, with other possibilities likely as well. For example, it has been shown that SR1664 exhibits its mechanism of antagonism by sterically clashing with Phe282 to destabilize the AF2 region, hindering the coactivator-binding capacity of the receptor (Marciano et al., 2015a). Both mechanisms result in the disruption of the AF2 surface, which appears to be a key factor in repressing transcription of target genes in PPARγ.

In summary, we present here the first report of an antagonist and inverse agonist conformation of H12 in PPARγ. Our crystal structures show that SR10171 and SR11023 induce an allosteric shift in H12, pulling it away from the ligand-dependent AF2 coactivator-binding face, which consequently abrogates transcriptionally promoting coactivator recruitment to the LBD. This shift in H12 conformation simultaneously enables corepressor recruitment through exposing the corepressor-binding pocket, to enable recruitment of transcriptionally suppressing corepressors to give SR10171 and SR11023 their non-activating properties. The mechanism by which H12 is allosterically shifted in PPARγ by the ligands is unique from other nuclear receptors, as H12 undergoes a tumble and trap motion, unseen in other nuclear receptors. This represents an exciting development toward understanding the mechanism of antagonism and inverse agonism in PPARγ, as well as aiding in further drug design to treat type 2 diabetes.

METHODS

All methods can be found in the accompanying Transparent Methods supplemental file.

SUPPLEMENTAL INFORMATION

Supplemental Information includes Transparent Methods and four figures and can be found with this article online at https://doi.org/10.1016/j.isci.2018.06.012.

AUTHOR CONTRIBUTIONS

J.B.B. and P.R.G. conceived and supervised the project. R.L.F. and J.B.B. performed crystallography experiments, crystallographic data processing, and analysis. A.C.M. contributed to crystallographic data processing. R.L.F. prepared protein samples for native mass spectrometry and native PAGE. R.L.F. performed native PAGE. T.L.P. performed native mass spectrometry and data analysis. A.-L.B. and T.M.K. performed chemical synthesis. R.L.F., T.L.P., A.C.M., P.R.G., T.M.K., and J.B.B. contributed to manuscript preparation.

DECLARATIONS OF INTERESTS

The authors declare no competing interests.

REFERENCES

Banks, A.S., McAllister, F.E., Camporez, J.P., Zushin, P.J., Jurczak, M.J., Laznik-Bogoslavski, D., Shulman, G.I., Gygi, S.P., and Spiegelman, B.M. (2015). An ERK/Cdk5 axis controls the diabetogenic actions of PPARgamma. Nature *517*, 391–395.

Bruning, J.B., Chalmers, M.J., Prasad, S., Busby, S.A., Kamenecka, T.M., He, Y., Nettles, K.W., and Griffin, P.R. (2007). Partial agonists activate PPARgamma using a helix 12 independent mechanism. Structure *15*, 1258–1271.

Brzozowski, A.M., Pike, A.C., Dauter, Z., Hubbard, R.E., Bonn, T., Engstrom, O., Ohman, L., Greene, G.L., Gustafsson, J.A., and Carlquist, M. (1997). Molecular basis of agonism and antagonism in the oestrogen receptor. Nature *389*, 753–758.

Chandra, V., Huang, P., Hamuro, Y., Raghuram, S., Wang, Y., Burris, T.P., and Rastinejad, F. (2008). Structure of the intact PPAR-gamma-RXR- nuclear receptor complex on DNA. Nature 456, 350–356.

Choi, J.H., Banks, A.S., Estall, J.L., Kajimura, S., Bostrom, P., Laznik, D., Ruas, J.L., Chalmers, M.J., Kamenecka, T.M., Bluher, M., et al. (2010). Anti-diabetic drugs inhibit obesity-linked phosphorylation of PPARgamma by Cdk5. Nature 466, 451–456.

Choi, J.H., Banks, A.S., Kamenecka, T.M., Busby, S.A., Chalmers, M.J., Kumar, N., Kuruvilla, D.S., Shin, Y., He, Y., Bruning, J.B., et al. (2011). Antidiabetic actions of a non-agonist PPARgamma ligand blocking Cdk5-mediated phosphorylation. Nature 477, 477–481.

Choi, S.S., Kim, E.S., Jung, J.E., Marciano, D.P., Jo, A., Koo, J.Y., Choi, S.Y., Yang, Y.R., Jang, H.J., Kim, E.K., et al. (2016). PPARgamma antagonist gleevec improves insulin sensitivity and promotes the browning of white adipose tissue. Diabetes 65, 829–839.

Chrisman, I.M., Nemetchek, M.D., de Vera, I.M.S., Shang, J., Heidari, Z., Long, Y., Reyes-Caballero, H., Galindo-Murillo, R., Cheatham, T.E., 3rd, Blayo, A.L., et al. (2018). Defining a conformational ensemble that directs activation of PPARgamma. Nat. Commun. 9, 1794.

DiRenzo, J., Soderstrom, M., Kurokawa, R., Ogliastro, M.H., Ricote, M., Ingrey, S., Horlein, A., Rosenfeld, M.G., and Glass, C.K. (1997). Peroxisome proliferator-activated receptors and retinoic acid receptors differentially control the interactions of retinoid X receptor heterodimers with ligands, coactivators, and corepressors. Mol. Cell. Biol. 17, 2166–2176.

Gampe, R.T., Jr., Montana, V.G., Lambert, M.H., Miller, A.B., Bledsoe, R.K., Milburn, M.V., Kliewer, S.A., Willson, T.M., and Xu, H.E. (2000). Asymmetry in the PPARgamma/RXRalpha crystal structure reveals the molecular basis of heterodimerization among nuclear receptors. Mol. Cell 5, 545–555.

Gelin, M., Delfosse, V., Allemand, F., Hoh, F., Sallaz-Damaz, Y., Pirocchi, M., Bourguet, W., Ferrer, J.L., Labesse, G., and Guichou, J.F. (2015). Combining 'dry' co-crystallization and in situ diffraction to facilitate ligand screening by X-ray crystallography. Acta Crystallogr. D Biol. Crystallogr. 71, 1777–1787.

Hamuro, Y., Coales, S.J., Morrow, J.A., Molnar, K.S., Tuske, S.J., Southern, M.R., and Griffin, P.R. (2006). Hydrogen/deuterium-exchange (H/D-Ex) of PPARgamma LBD in the presence of various modulators. Protein Sci. 15, 1883–1892.

Hughes, T.S., Chalmers, M.J., Novick, S., Kuruvilla, D.S., Chang, M.R., Kamenecka, T.M., Rance, M., Johnson, B.A., Burris, T.P., Griffin, P.R.,

et al. (2012). Ligand and receptor dynamics contribute to the mechanism of graded PPARgamma agonism. Structure 20, 139–150.

Issemann, I., Prince, R.A., Tugwood, J.D., and Green, S. (1993). The retinoid X receptor enhances the function of the peroxisome proliferator activated receptor. Biochimie 75, 251–256.

Johnson, B.A., Wilson, E.M., Li, Y., Moller, D.E., Smith, R.G., and Zhou, G. (2000). Ligand-induced stabilization of PPARgamma monitored by NMR spectroscopy: implications for nuclear receptor activation. J. Mol. Biol. 298, 187–194.

Khandekar, M.J., Banks, A.S., Laznik-Bogoslavski, D., White, J.P., Choi, J.H., Kazak, L., Lo, J.C., Cohen, P., Wong, K.K., Kamenecka, T.M., et al. (2018). Noncanonical agonist PPARgamma ligands modulate the response to DNA damage and sensitize cancer cells to cytotoxic chemotherapy. Proc. Natl. Acad. Sci. USA 115, 561–566.

Kojetin, D.J., Matta-Camacho, E., Hughes, T.S., Srinivasan, S., Nwachukwu, J.C., Cavett, V., Nowak, J., Chalmers, M.J., Marciano, D.P., Kamenecka, T.M., et al. (2015). Structural mechanism for signal transduction in RXR nuclear receptor heterodimers. Nat. Commun. 6, 8013.

Kroker, A.J., and Bruning, J.B. (2015). Review of the structural and dynamic mechanisms of PPARgamma partial agonism. PPAR Res. 2015, 816856.

Liberato, M.V., Nascimento, A.S., Ayers, S.D., Lin, J.Z., Cvoro, A., Silveira, R.L., Martinez, L., Souza, P.C., Saidemberg, D., Deng, T., et al. (2012). Medium chain fatty acids are selective peroxisome proliferator activated receptor (PPAR) gamma activators and pan-PPAR partial agonists. PLoS One 7, e36297.

Liko, I., Allison, T.M., Hopper, J.T., and Robinson, C.V. (2016). Mass spectrometry guided structural biology. Curr. Opin. Struct. Biol. 40, 136–144.

Marciano, D.P., Kuruvilla, D.S., Boregowda, S.V., Asteian, A., Hughes, T.S., Garcia-Ordonez, R., Corzo, C.A., Khan, T.M., Novick, S.J., and Park, H. (2015a). Pharmacological repression of PPAR [gamma] promotes osteogenesis. Nat. Commun. 6, 7443.

Marciano, D.P., Kuruvilla, D.S., Pascal, B.D., and Griffin, P.R. (2015b). Identification of Bexarotene as a PPARgamma antagonist with HDX. PPAR Res. 2015, 254560.

Nolte, R.T., Wisely, G.B., Westin, S., Cobb, J.E., Lambert, M.H., Kurokawa, R., Rosenfeld, M.G., Willson, T.M., Glass, C.K., and Milburn, M.V. (1998). Ligand binding and co-activator assembly of the peroxisome proliferator-activated receptor-gamma. Nature 395, 137–143.

Pike, A.C., Brzozowski, A.M., Hubbard, R.E., Bonn, T., Thorsell, A.G., Engstrom, O., Ljunggren, J., Gustafsson, J.A., and Carlquist, M. (1999). Structure of the ligand-binding domain of oestrogen receptor beta in the presence of a partial agonist and a full antagonist. EMBO J. 18, 4608–4618.

Shiau, A.K., Barstad, D., Loria, P.M., Cheng, L., Kushner, P.J., Agard, D.A., and Greene, G.L. (1998). The structural basis of estrogen receptor/coactivator recognition and the antagonism of this interaction by tamoxifen. Cell 95, 927–937.

Srinivasan, S., Nwachukwu, J.C., Bruno, N.E., Dharmarajan, V., Goswami, D., Kastrati, I., Novick, S., Nowak, J., Cavett, V., Zhou, H.B., et al. (2017). Full antagonism of the estrogen receptor without a prototypical ligand side chain. Nat. Chem. Biol. 13, 111–118.

Stechschulte, L.A., Czernik, P.J., Rotter, Z.C., Tausif, F.N., Corzo, C.A., Marciano, D.P., Astean, A., Zheng, J., Bruning, J.B., Kamenecka, T.M., et al. (2016). PPARG post-translational modifications regulate bone formation and bone resorption. EBioMedicine 10, 174–184.

Taygerly, J.P., McGee, L.R., Rubenstein, S.M., Houze, J.B., Cushing, T.D., Li, Y., Motani, A., Chen, J.L., Frankmoelle, W., Ye, G., et al. (2013). Discovery of INT131: a selective PPARgamma modulator that enhances insulin sensitivity. Bioorg. Med. Chem. 21, 979–992.

van Marrewijk, L.M., Polyak, S.W., Hijnen, M., Kuruvilla, D., Chang, M.R., Shin, Y., Kamenecka, T.M., Griffin, P.R., and Bruning, J.B. (2016). SR2067 reveals a unique kinetic and structural signature for PPARgamma partial agonism. ACS Chem. Biol. 11, 273–283.

Wakabayashi, K., Hayashi, S., Matsui, Y., Matsumoto, T., Furukawa, A., Kuroha, M., Tanaka, N., Inaba, T., Kanda, S., Tanaka, J., et al. (2011). Pharmacology and in vitro profiling of a novel peroxisome proliferator-activated receptor gamma ligand, Cerco-A. Biol. Pharm. Bull 34, 1094–1104.

Xu, H.E., Stanley, T.B., Montana, V.G., Lambert, M.H., Shearer, B.G., Cobb, J.E., McKee, D.D., Galardi, C.M., Plunket, K.D., Nolte, R.T., et al. (2002). Structural basis for antagonist-mediated recruitment of nuclear co-repressors by PPARalpha. Nature 415, 813–817.

Zheng, J.C., C, Chang, M., Sang, J., Lam, V., Brust, R., Blayo, A., Bruning, J., Kamenecka, T., Kojetin, D., and Griffin, P. (2018). Chemical crosslinking mass spectrometry reveals the conformational landscape of the activation helix of PPARγ; a model for ligand-dependent antagonism. Structure. Published online May 23, 2018, in press.